L_2^+, an Improved Line of Sight Guidance Law for UAVs

Renwick Curry[1], Mariano Lizarraga[2], Bryant Mairs[3], and Gabriel Hugh Elkaim[4]

Abstract—

This paper describes a new guidance law that extends the line-of-sight guidance law previously developed by Park *et al*. Several improvements are presented that allow operation in the real world. A stability analysis accounts for the dynamic response of the bank angle commands which leads to the definition of regions of instability. Another extension accounts for situations where the cross-track error is larger than the lookahead distance. Another modifies the lookahead distance so that the transient response is independent of ground speed. Yet another extension defines a "homing" mode in which the UAV flies to a goal point without a defined path, commonly used as a "return-to-base," either as a safety measure or as an end-of-mission order. Since there is no constraint that the goal point be stationary, we demonstrate that the new law can be used to follow a moving target whose location is known, such as a mobile ground control station. Simulations with a 6 degree of freedom aircraft model demonstrate these features.

I. INTRODUCTION

A. Overview

UAVs span a wide range in size and complexity. The largest UAVs, such as Predator or Globalhawk, can weigh several thousand pounds and have wing spans on the order of 10 to 100 feet. Regardless of their size and mission, all UAVs share the need for Guidance, Navigation and Control (GNC) systems. This work focuses on the guidance system: the guidance system takes into account the UAV's state and, based on the currently defined mission, generates the state trajectory the UAV should follow in accomplishing its mission. Thus, it is this key component inside the UAV that enables the ground operator to issue high-level commands, such as "fly to this location" or "follow this line". Ultimately, these systems allow the vehicle to follow a desired trajectory to complete its mission.

B. Related Work

There is a wide variety of UAV guidance laws reported in the literature for path following. Kaminer *et. al.* [1] describes an integrated approach. Niculescu [2] describes a navigation system designed to track straight lines between waypoints. It aims the ground track at a point along the desired straight line, a point defined as a fraction of the distance remaining. A recent innovation is the use of vector fields[3][4], wherein a velocity field is specified over space and the vehicle's ground track is commanded to follow these velocity vectors. Stability for tracking straight lines, circular arcs, and circular paths is shown. Rhee *et al.* [5] take advantage of the predefined

Department of Computer Engineering, University of California Santa Cruz, Santa Cruz, CA 95064, USA
[1]rcurry@ucsc.edu, [2]malife@gmail.com,
[3]bwmairs@ucsc.edu, [4]elkaim@soe.ucsc.edu

path by another method. They fit cubic splines to the path, and feed the required lateral acceleration forward to the bank angle control system. Path following errors are further corrected by a PID controller wrapped around the vehicle's response to the feedforward acceleration command.

Other guidance techniques borrow from algorithms originally developed for missile guidance. That said, the genesis of one popular technique was developed for ground robots [6]. In this technique the lateral acceleration is commanded to follow a circular path back to the reference path. When applied to UAVs by Park *et al.*[7][8], the result is the same as pursuit tracking originally used for air-to-air missiles, except that the "target" is always at a fixed range. Lyapunov stability is proven for tracking circular paths and straight lines with this method assuming the lateral acceleration response to commands is instantaneous. Importantly, none of these techniques account for the response time of the bank angle to commanded acceleration. As we will see, this lag can cause instability.

This paper discusses the guidance law as implemented in the SLUGS autopilot [9]. It shares all the advantages of the pursuit guidance presented in Ref. [8], namely, the elegance and simplicity of the solution and the low demand for computing-power. But we add several extensions required for operational environments, e.g. defining aim points for all flight conditions not treated by [8]. Furthermore, the linearized analysis of [8] is extended to incorporate the roll dynamics of the UAV to show conditions which lead to instability of the original logic, e.g., certain combinations of roll response lag and fluctuations in ground speed, conditions which do occur in practice. The guidance logic presented here differs by having its performance and stability be independent of the ground speed, In addition, we have included a "homing" mode using the same guidance logic in which the UAV flies to a goal point without a predefined path. This mode is useful for "return-to-base" (RTB) at the end of a mission, in case of communications failure, or to fly to a specified point before entering a waypoint array. There is no requirement that the goal point be stationary and this logic has successfully been used to track a moving target.

C. Paper Outline

The rest of this paper is structured as follows: Section II presents a brief overview of the nonlinear guidance law as presented in Ref. [8]. Section III contains a stability analysis of the linearized system including roll response dynamics. Section IV introduces the proposed guidance law and discusses its improvements. Section V contains the
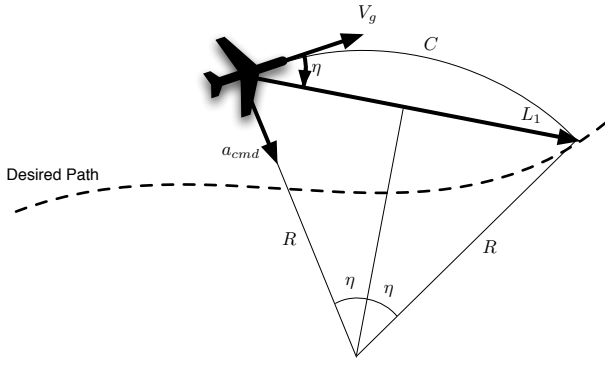
Fig. 1: Line of sight geometry. After Fig. 1 in Ref. [7]

results of simulations comparing the proposed guidance logic with the original, and Section VI is a summary.

II. LINE OF SIGHT GUIDANCE

The guidance law discussed later in this paper follows closely from that first presented by Amidi [6] for ground vehicles then applied to UAVs and analyzed extensively by Park, Deyst, and How [7], [8]. These papers describe the guidance law to generate lateral acceleration commands to track arbitrary paths. This section briefly presents the guidance law as derived in Ref. [8].

Conceptually, this guidance law steers the velocity vector toward the line of sight to an aim point, and thus is a form of pursuit guidance originally used in air-to-air missiles. For the remainder of the paper, we refer to this as L_1 guidance based on the authors' notation for the look ahead distance in [8] and it is *not* related to the well-known $\mathcal{L}_1$ norm.

Based on the geometry shown in Fig. 1, let V_g be the UAV's horizontal velocity vector with respect to the ground and C be a circular arc of radius R that lies tangent to the velocity vector and passing through the UAV position.

Let L_1 be a constant lookahead distance from the UAV position to the path in the desired direction of travel. The circular arc C passes through the intersection of this distance with the desired path and is fully described by its two end points and radius R. This L_1 vector is divided into two equal segments by the line that bisects the chord defined by the circular arc C. Then from elementary trigonometry:

$$\frac{|L_1|}{2} = R \sin \eta. \tag{1}$$

Additionally, from elementary kinematics it is known that the centripetal acceleration, a_c, required to follow the circular arc C is given by:

$$a_c = \frac{|V_g|^2}{R}. \tag{2}$$

Therefore to follow the arc C the UAV must command a lateral acceleration of a_c. Solving Eq. 1 for R and substituting it into Eq. 2 produces the following guidance law for commanded acceleration:

$$a_{cmd} = 2\frac{|V_g|^2}{|L_1|} \sin \eta. \tag{3}$$

It is clear that the only requirements for the implementation of this control law are to select the lookahead distance $|L_1|$ and to determine $\sin \eta$, where η is the angle from the velocity vector to L_1, sometimes referred to as the line of sight angle. $|L_1|$ is analogous to feedback gain, with a larger L_1 corresponding to smaller gains.

The quantity $\sin \eta$ is found from the vector cross product of V_g and L_1.

$$\sin \eta = \frac{V_g \times L_1}{|V_g||L_1|}. \tag{4}$$

For the UAV to actually track the desired trajectory, the lateral acceleration command, a_{cmd}, computed in Eq. 2 must be converted to an appropriate bank angle command ϕ_{cmd} using the steady-state turn equation for an aircraft:

$$\phi_{cmd} = \tan^{-1}\left(\frac{a_{cmd}}{g}\right). \tag{5}$$

III. LINEARIZED ANALYSIS WITH ROLL DYNAMICS

A. L_1 Transfer Function

A small angle analysis of the L_1 guidance logic is presented in [8] using the notation in Fig. 2 adapted from that paper.
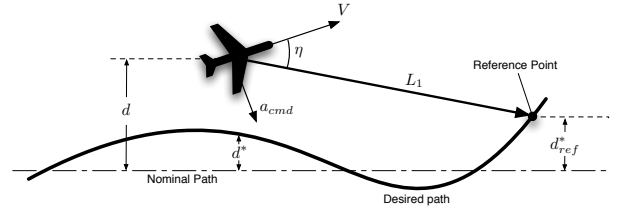

Fig. 2: L_1 guidance for an arbitrary path. After Fig. 3 in Ref. [8]

The authors show that the following transfer function describes the response of the system:

$$\frac{d}{d_{ref}} = \frac{\omega_n^2}{s^2 + 2\zeta\omega_n s + \omega_n^2}, \tag{6}$$

where

$$\begin{aligned} \zeta &= 0.707, \\ \omega_n &= \sqrt{2}\frac{|V_g|}{|L_1|}. \end{aligned} \tag{7}$$

Note that the pole location depends only on $|L_1|/|V_g|$, so we use the following symbol for this characteristic system time

$$\frac{|L_1|}{|V_g|} \equiv T \tag{8}$$

B. Bank Angle Response

The Lyapunov stability analysis in Ref. [8] assumes actual lateral acceleration is the same as commanded acceleration, i.e., roll angle response is instantaneous. However, our simulations with a six degree of freedom aircraft model showed bank angle response to be long enough that the guidance logic had to be modified in several ways. More instability

was observed in flight than expected from the linearized analysis of [8].

The block diagram (shown in Fig. 3) is used to explore the effects of roll dynamics. Roll dynamics can be modeled approximately as a first order lag from the fact that lateral acceleration is a function of bank angle as shown in Eq. 5.
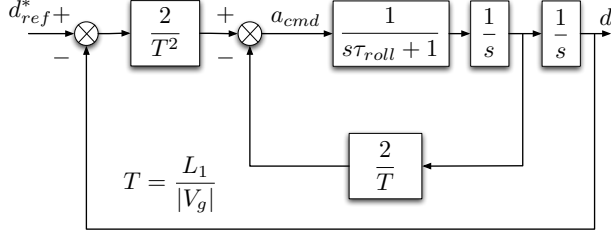

Fig. 3: Block Diagram of L1 Guidance with Roll Dynamics

In this diagram the definition for T is from Eq. 8 and τ_{roll} as the first order time constant of the roll angle response to roll commands.

A root locus can be constructed for various values of T using the characteristic equation for the system:

$$\frac{T^2 \tau_{roll}}{2}s^3 + \frac{T^2}{2}s^2 + Ts + 1 = 0 \qquad (9)$$

The root locus of Fig. 4 constructed for $T = 0.5 : 0.5 : 10$ clearly shows system instability for smaller values of T. In fact it can be shown that the system is marginally stable when $T = \tau_{roll}$. Moreover, this occurs at the frequency $\omega = \sqrt{\frac{2}{T\tau_{roll}}}$. Thus it is important to ensure that $T > \tau_{roll}$ at all times. Niculescu [2] noted this instability empirically during simulations with a 6 degree-of-freedom aircraft model, but did not explore it further.
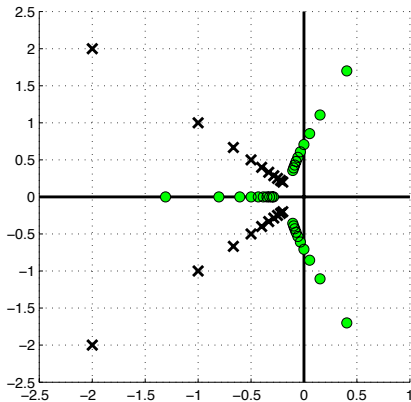

Fig. 4: Root Locus without roll dynamics ($\tau_{roll} = 0$, $\times$ symbol) and with roll dynamics ($\tau_{roll} = 2$, green circle). Poles migrate away from the origin as T decreases (V_g increases)

IV. L_2^+ GUIDANCE LAW

A. Lookahead Distance

To be useful for the many conditions that occur in real flight operations, the L_1 guidance law must be extended. The extension address the fact that the L_1 intercept can be undefined. The overall theme is to *always* define an aim point, regardless of flight state or mission. The notation L_2^+ is used to denote the revised algorithm with these modifications and extensions.

The first change to Eq. 3 was precipitated by an observation of the large overshoot in waypoint switching when leaving a downwind leg. Reduced stability was also noticed when tracking on downwind legs. To alleviate this, the look ahead distance, L_1, was changed so that the pole location became independent of groundspeed: this was done by modifying Eq. 8 to calculate the look ahead distance as a function of groundspeed:

$$|L_2| = T^*|V_g| \qquad (10)$$

where T^* is a constant. Now the natural frequency of the linearized response becomes $\sqrt{2}/T^*$, which is independent of ground speed. Given the results of the root locus analysis, it is shown that T^* should be chosen to be at least 3 to 4 times the roll response lag τ_{roll} to ensure satisfactory transient response.

Substituting Eq. 10 into Eq. 3 provides the guidance law for L_2^+:

$$a_{cmd} = 2\frac{|V_g|}{T^*}\sin\eta. \qquad (11)$$

B. Aim Point Definition

Another limitation of L_1 guidance is that the lateral acceleration is undefined when the UAV is farther than L_1 from the desired track, because the normal aim point (the intersection of the desired path and L_1) is not defined. This can occur because the lateral error becomes very large during normal tracking, or because the guidance logic has just been activated and the UAV is far from the desired trajectory. To enforce the existence of an aim point in the L_2^+ guidance logic, the following rules are used when the UAV is farther than $|L_2|$ away from the desired track:

- **Maximum Intercept Angle**: Large intercept angles lead to large overshoot when first acquiring the desired path, so the aim point is defined by the maximum intercept angle γ typically 45 degrees.
- **Along Track Distance**: Here the aim point is defined by the distance towards the active waypoint. To preserve generality and scalability, we define the distance as a constant, $\mathcal{M}^*$, times the lookahead distance $|L_2|$.
- **Aim Point**: The waypoint is defined to be at the smaller of these two down-path distances as shown in Fig. 5. This allows rapid acquisition of the track when the lateral error is large, yet limits the intercept angle as this error becomes smaller.
- **Maximum Down Track Distance**: Even with the above limitation on the down path distance, the aim point
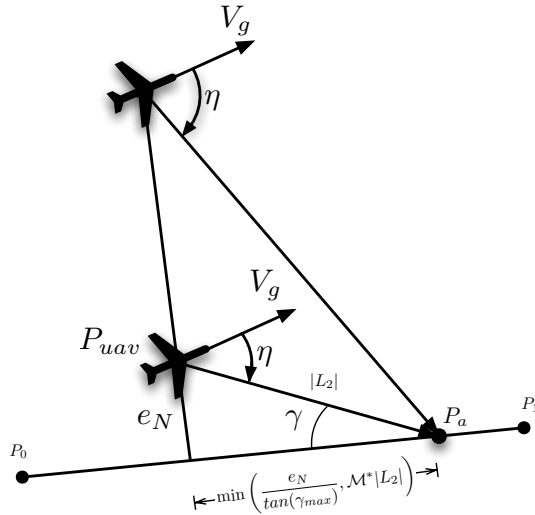
Fig. 5: L_2^+ Aim point definition

could lie beyond the active waypoint or due to the position of the UAV. Proper tracking is obtained by further limiting the down path aim point to be on the active leg but at or before the active waypoint.

C. Bank Angle Limit

The acceleration command is computed as in Eq. 11, where $\sin \eta$ is obtained from Eq. 4. Note that it is possible that the aircraft's groundspeed is in a direction such that η is 90° or more. In these cases, a maximum lateral acceleration, a_{max}, was used to avoid extreme angle commands in cases where the line-of-sight angle is near 90°. In addition, the maximum acceleration should be used for $\eta > 90°$ to improve response time. Therefore, we used:

$$a_{max} = g \tan \phi_{max} \tag{12}$$

where ϕ_{max} is a predefined constant. This implies a limit on η when computing commanded acceleration by Eq. 11. This limit is found by equating Eq. 11 and 12 and yields:

$$\eta_{max} = sin^{-1}\left(\frac{T^* g \tan \phi_{max}}{2V_g}\right) \tag{13}$$

With this limitation the bank angle command becomes:

$$\phi_{cmd} = \begin{cases} -\phi_{max} & \eta \leq -\eta_{max} \\ tan^{-1}\left(2\frac{|V_g|}{gT^*}\sin \eta\right) & |\eta| < \eta_{max} \\ \phi_{max} & \eta \geq \eta_{max} \end{cases} \tag{14}$$

D. Waypoint Switching

The desired path near a waypoint is very mission specific. For example, the path may be constrained to fly "near" the waypoint, overfly the waypoint, or fly one or more circles around the waypoint. Either the trajectory can be specified throughout, e.g., circular or other paths to accomplish the mission, or left unspecified. In the unspecified case, the path itself is not defined, only the points at which the UAV switches from one leg (defined as the line between two successive waypoints) to the next leg are defined.

Often a curved path or circular arc is used to connect two legs at a waypoint, thus resulting in a trajectory with two straight lines joined by a curve. Ideally, the UAV should be able to fly the entire path without error, and to some extent this can be handled by feedforward. However, at the curved section the L_1 logic will cause the UAV to deviate from the straight line segment when the aim point is on the curved path even though the UAV should still be tracking the straight path. That is, the transition to the curved path lies in between the two ends of the L_1 vector. This is illustrated in Fig. 6 which shows a circular path tangent to the two path legs. The points of tangency are at a distance p from the waypoint:

$$p = \frac{R}{\tan \delta} \tag{15}$$

$$\delta = \frac{\pi - \Gamma}{2}, \tag{16}$$

where Γ is the angle of the course change, and R is the radius of the circle. The figure shows how the L_1 vector
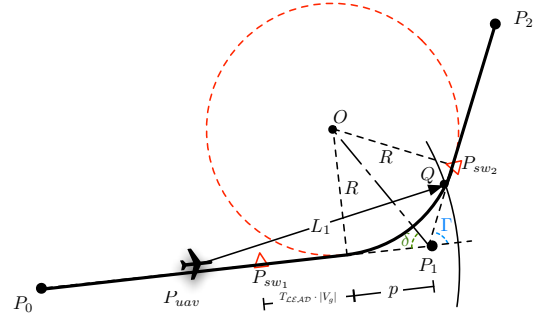

Fig. 6: Waypoint switching geometry showing the circular arc connecting two legs.

has started tracking the circular path when the tip of the L_1 vector reached the tangency point and now intersects the circular path at point Q. This will lead to deviations from the desired path (solid line) before reaching the tangency point p. To avoid this premature tracking of the curved path, the aim point is altered to track the straight line until the *projection* of the UAV's position on the path reaches the curved path. When the projection of the UAV's position is at the end of the curved path (point P_{sw2}) straight line tracking resumes.

In the UAV application, we found that initiating the turn just at the point of tangency p, was not adequate because of the lag time of the roll control system. Therefore we introduced the concept of a lead time $\mathcal{T}_{\mathcal{LEAD}}$ to initiate the turn. When this lead time is multiplied by the groundspeed, it gives the extra distance from the waypoint to the switch point. The new switch point distance becomes:

$$P_{sw1} = \mathcal{T}_{\mathcal{LEAD}}|V_g| + p. \tag{17}$$

A lead time was necessary to compensate for the bank angle response time by some specified fixed time $\mathcal{T}_{\mathcal{LEAD}}$ regardless of the waypoint transition path used.

E. Homing

There are cases where no reference path is available, yet a goal (aim point) does exist. An important example is "return to base" (RTB) function which is activated when communications are lost, when a failure occurs, or when the mission is over.

Another situation arises when it is desired to pass through an array of waypoints in a consistent manner but the initial position of the UAV may be anywhere, even beyond the array of waypoints. In this case it helps to first fly to an "Initial Point," much like that used in piloted instrument landings. This point is placed so that a consistent approach to the waypoints always happens.

A third application of a goal without a path occurs when the UAV is following/tracking a moving vehicle. Again, there is a well defined goal (the followed vehicle) but no well defined path.

The L_2^+ logic includes a homing mode, whereby the goal becomes the aim point (e.g., base, initial point, moving target). In this mode the lateral acceleration is still computed according to Eq. 11. Upon reaching the goal, the UAV will continue to fly towards the aim point in accordance to Eq. 11, resulting in the UAV continually orbiting the aim point.

V. SIMULATIONS

All the results in this section used the switching point of Eq. 17 to determine when to change active waypoints. At that point the line tracking logic of L_2 was used to acquire and track the line to the newly activated waypoint.

A. Roll Dynamics

Section III showed how the roll dynamics impact system stability for smaller values of $T = \frac{L_1}{|V_g|}$. For these simulations, and in order to make the L_1 and L_2^+ controllers comparable, the commanded airspeed, U_{cmd}, was $16m/s$, and T^* was set to 3.5 for the L_2^+ logic. For the L_1 logic, the lookahead distance, L_1, was set to $3.5 \times U_{cmd}$. With these parameters in a zero wind case, $L_1 = L_2$. Fig. 7 and 8 demonstrate the two algorithms for the case that the mean wind is $8m/s$ from the East (right to left) with a white noise component of $1m/s$ in all directions. The green square in Fig. 7 is the initial point.

When the UAV is on a downwind leg $T = |L_1|/|V_g|$ is reduced because of the increase in groundspeed. The stability analysis presented in Sec. III showed decreasing stability as T grows smaller. This phenomenon is evident in Fig. 7 because of the increase in groundspeed going from waypoint 1 to waypoint 2 and in the transition from waypoint 4 to waypoint 5. The same effect is seen in Fig. 8 en route to the circle, and on the downwind side of the circle. The growth in oscillations is due to the excitation of the random winds. Note that L_2^+ guidance does not show these effects because the pole locations are independent of ground speed.

B. Return To Base (RTB)

The homing logic used in the initial point and return to base is shown in Fig. 9. The UAV starts at the base (red
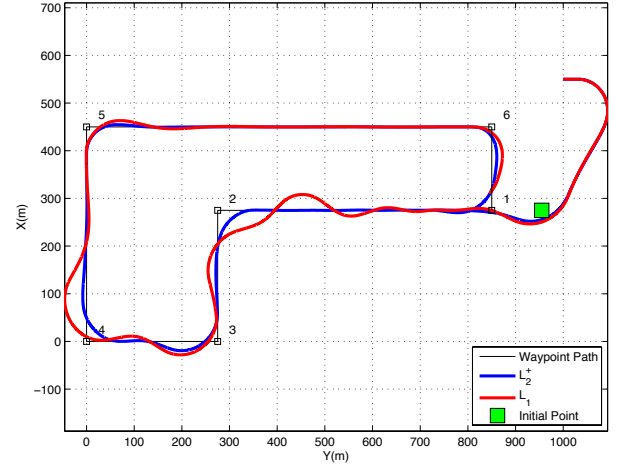

Fig. 7: Waypoint tracking with wind. Airspeed = 16m/s, mean wind=$8m/s$ from 090 (right to left)
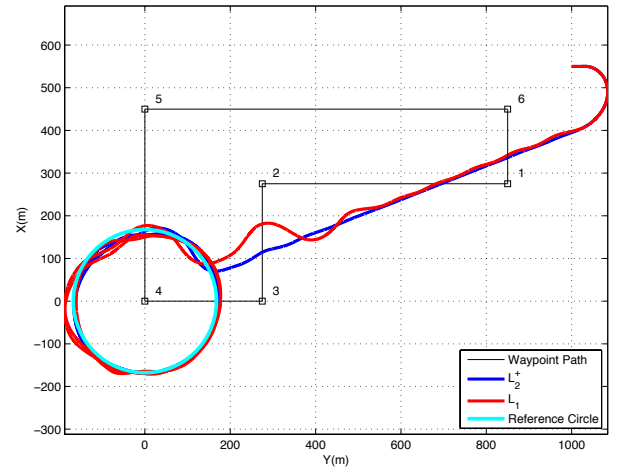

Fig. 8: Circle tracking with wind. Airspeed = 16m/s, mean wind=8m/s from 090 (right to left)

circle) and proceeds directly to the initial point (green square) and then into the waypoint array.

The tangent circles at each waypoint were used to determine the switching points (inverted triangles in Fig. 6). When the change in course angle is very large, as it is for waypoint 3, the transition circle can be far removed from the UAV when that waypoint becomes active. The tangent circle for waypoint 3 is just south of waypoint 4 in Fig. 9. In these cases, the switching logic skips the waypoint and the next waypoint immediately becomes active.

The RTB signal causes the homing logic to be activated between waypoints 4 and 1, and the UAV returns to base. The homing logic is never turned off, so after passing over the base the UAV begins an immediate turn back to the base, resulting in an orbiting pattern. The exact orbiting pattern depends on environmental conditions and the UAV track as it approaches the base.
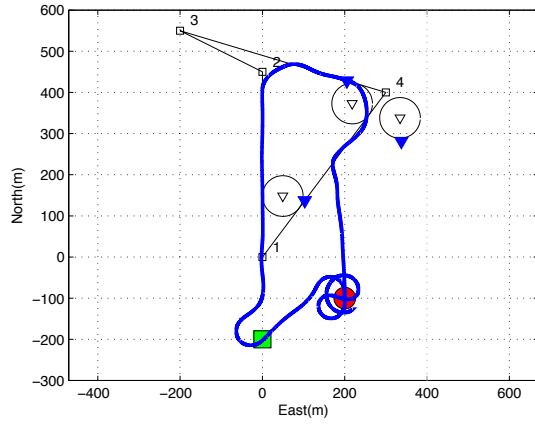
Fig. 9: Waypoint tracking and return to base. Red circle is the base; green square is the Initial Point.

Fig. 10: RTB logic applied to moving base. Green track is a 3 second prediction of base position. Wind is from the east.

C. Moving Base

Fig. 10 shows the ground tracks of a moving base and the UAV. The reported position of the base was filtered with a $1rad/s$ low pass filter, and the rate of this filtered output was used to create a 3 second prediction of the vehicle position. The predicted position was the input to the homing logic without any further modification to the homing logic. The commanded airspeed was $16m/s$, the wind was $5m/s$ from the east, blowing right to left. The base moved at $10m/s$. On the downwind leg (North 480m) the groundspeed of the UAV was more than double that of the base so some delaying maneuvers were required. The homing logic caused the UAV to overtake the base and make a series of maximum bank turns to return to the base which had already moved on. On the eastbound legs (North 750m), the excess ground speed was only $1m/s$, so no delaying maneuvers were required. Instead, the UAV approached the moving base asymptotically, having lost ground at the previous turn.

It can be seen in Fig. 10 that the UAV flew circular turns when the base changed direction two times at (East -220m). In each case the UAV had just overflown the prediction point and the homing logic commanded a maximum banked turn to the left, just before the moving base turned to the right. Once in a maximum bank angle turn, the commanded turn rate does not change sign unless $\sin\eta$ also changes sign, even if the commanded turn is causing η to grow larger, as it is in this case.

VI. SUMMARY

This work describes extensions of the pursuit guidance law presented in Ref. [8]. This new guidance shares all the the elegance and simplicity of the L_1 guidance law and at the same time accounts for cases regularly encountered in operational environments: e.g. defining aim points for all flight conditions not treated in the original work. A stability analysis was performed which incorporated the roll dynamics of the UAV. This analysis showed conditions leading to marginal stability of the original logic. Particularly under certain combinations of roll response and ground speed,
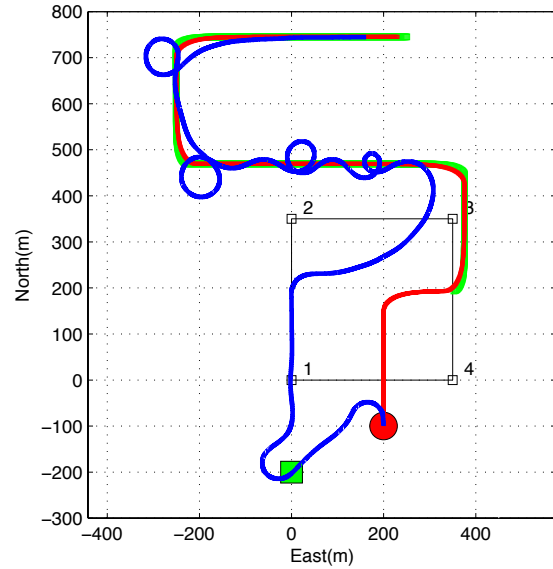
which do occur in practice. The stability analysis was used to choose the lookahead distance not as a fixed distance, but as a constant lookahead time such that the poles of the linearized system are independent of the ground speed. In addition, a "homing" mode was defined using the same guidance logic in which the UAV flies to goal point without a predefined path. This mode is useful for "return-to-base" at the end of a mission or for following a moving ground target. The results of these additions to the original pursuit guidance, now called L_2^+, are demonstrated in simulations with a high-fidelity 6DOF aircraft model.

REFERENCES

[1] I. Kaminer, A. Pascoal, E. Hallberg, and C. Silvestre, "Trajectory tracking for autonomous vehicles: An integrated approach to guidance and control," *AIAA J. Guidance ontorl, and Dynamics*, vol. 21, no. 1, pp. 29–38, 1998.

[2] M. Niculescu, "Lateral track control law for aerosonde uav," vol. 39th AIAA Aeospaces Sciences Meeting and Exhibit, Jan 2001.

[3] D. Nelson, B. Barber, T. McLaon, and R. Beard, "Vector field path following for miniature air vehicles," *IEEE Trans. on Robotics*, vol. 23, no. 3, pp. 519–529, June 2007.

[4] T. Summers, M. Akella, and M. Mears, "Coordinated standoff tracking of moving targets: Control laws and information arcchitectures," *Journal of Guidance, Control and Dynamics*, vol. 32, no. 1, pp. 57–69, 2009.

[5] P. S. Rhee, I. and C.-K. Ryoo, "A tight path following algorithm of an uas based on pid control," in *SICE Annual Conference*. SICE, August 18-21 2010.

[6] O. Amidi and C. Thorpe, "Integrated mobile robot control," in *Proc. SPIE*, vol. 1388, no. 504, 1991.

[7] S. Park, J. Deyst, and J. How, "A new nonlinear guidance logic for trajectory tracking," Jan 2004.

[8] S. Park, J. Deyst, and J. P. How, "Performance and Lyapunov stability of a nonlinear path-following guidance method," *Journal of Guidance, Control and Dynamics*, vol. 30, no. 6, p. 1718, 2007.

[9] M. Lizarraga, "Design, implementation and flight verification of a versatile and rapidly reconfigurable uav gnc research platform," Ph.D. dissertation, Department of Computer Engineering, University of California Santa Cruz, Santa Cruz, CA, December 2009.